International Journal of Applied Earth Observations and Geoinformation 108 (2022) 102756

Contents lists available at ScienceDirect

International Journal of Applied Earth Observations and Geoinformation

journal homepage: www.elsevier.com/locate/jag

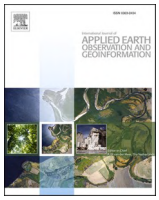

Multi-technique geodetic detection of onshore and offshore subsidence along the Upper Adriatic Sea coasts

Marco Polcari, Valeria Secreti, Letizia Anderlini, Matteo Albano, Mimmo Palano, Enrico Serpelloni, Salvatore Stramondo, Elisa Trasatti, Giuseppe Pezzo *

Istituto Nazionale di Geofisica e Vulcanologia, Via di Vigna Murata 605, I-00143 Rome, Italy

ARTICLE INFO

Keywords:
InSAR
GNSS
Leveling
Lido di Dante
Cross-Validation
Onshore and offshore deformation

ABSTRACT

We assess about 20 years of onshore and offshore subsidence along a sector of the Upper Adriatic Sea (Italy) coastal areas affected by natural soil compaction and intense anthropogenic activities such as aquifers exploitation and hydrocarbons extraction. Our approach is based on the synergistic use of independent remote sensing and in-situ geodetic data to detect and spatially characterise the deformation pattern by cross-validating the different available measurements. We collect extensive datasets from i) SAR images provided by Envisat, CosmoSkyMed and Sentinel-1 missions, ii) GNSS measurements from continuous stations managed by public institutions, local authorities and private companies and iii) Leveling surveys. The cross-validation analysis shows good agreement among all the independent datasets, thus providing a reliable assessment of the ongoing deformation. We detect an onshore and offshore subsidence peak of about −1/-1.5 cm/yr in the proximity of the coastline, close to Lido di Dante and Fiumi Uniti villages, and at the present offshore platform. The outcomes highlight how the integration of different remote sensing and in situ geodetic techniques is successful to retrieve deformation history in time and space in complex areas, where different natural and anthropogenic sources concur to the overall deformation pattern. Moreover, such approach provides a robust support to modelling studies for hazard assessment in both inland and shoreline areas.

1. Introduction

Northern Italy coastal areas are historically affected by several land subsidence processes induced by natural and anthropogenic phenomena (Teatini et al., 2005). Indeed, the soft sediments characterizing the Po Plain are prone to natural compaction effects of the order of few mm/year (Gambolati and Teatini, 1998). In addition, from the end of the Second World War, these areas were also interested by extensive groundwater withdrawals for civil, industrial and agricultural purposes that significantly contributed to the land subsidence with rates in the order of some cm/year (Gonella et al., 1998; Teatini et al., 2006).

Furthermore, starting from the second half of the 20th century, many oil and natural gas reservoirs were discovered and several concessions granted to different companies for sub-soil mineral resources exploitation activities along both onshore and offshore sites. Then, due to the combined effect of these anthropogenic and natural processes, many areas experienced a further increase of land subsidence which could impact, synergistically with sea level rise, the coastline evolution (Gambolati et al., 1999) and need to be monitored carefully.

In this context, combined remote sensing and in-situ techniques such as Synthetic Aperture Radar Interferometry (InSAR), Global Navigation Satellite System (GNSS) and Leveling surveys are largely exploited, providing spatially dense and accurate ground deformation measurements, that can support the estimation of the different contributions to subsiding areas (Vasco et al., 2002; Klemm et al., 2010; Montuori et al., 2018).

In this work, we collect and analyse a large multi-source dataset consisting of InSAR, GNSS and Leveling data to reconstruct the temporal and spatial evolution of about 20 years of onshore and offshore subsidence along a sector of the Upper Adriatic Sea coastal area interested by subsidence phenomena. Our goal is to provide a quantitative and reliable assessment of the ground displacement by a cross-validation procedure between the measurements from different data sources.

The study area encompasses a coastal region of approximately 400 km^2 east of Ravenna city where severe ground subsidence has been documented in the past (Bitelli et al., 2000; Carminati & Martinelli,

* Corresponding author.
E-mail address: Giuseppe.pezzo@ingv.it (G. Pezzo).

https://doi.org/10.1016/j.jag.2022.102756
Received 8 November 2021; Received in revised form 28 February 2022; Accepted 21 March 2022

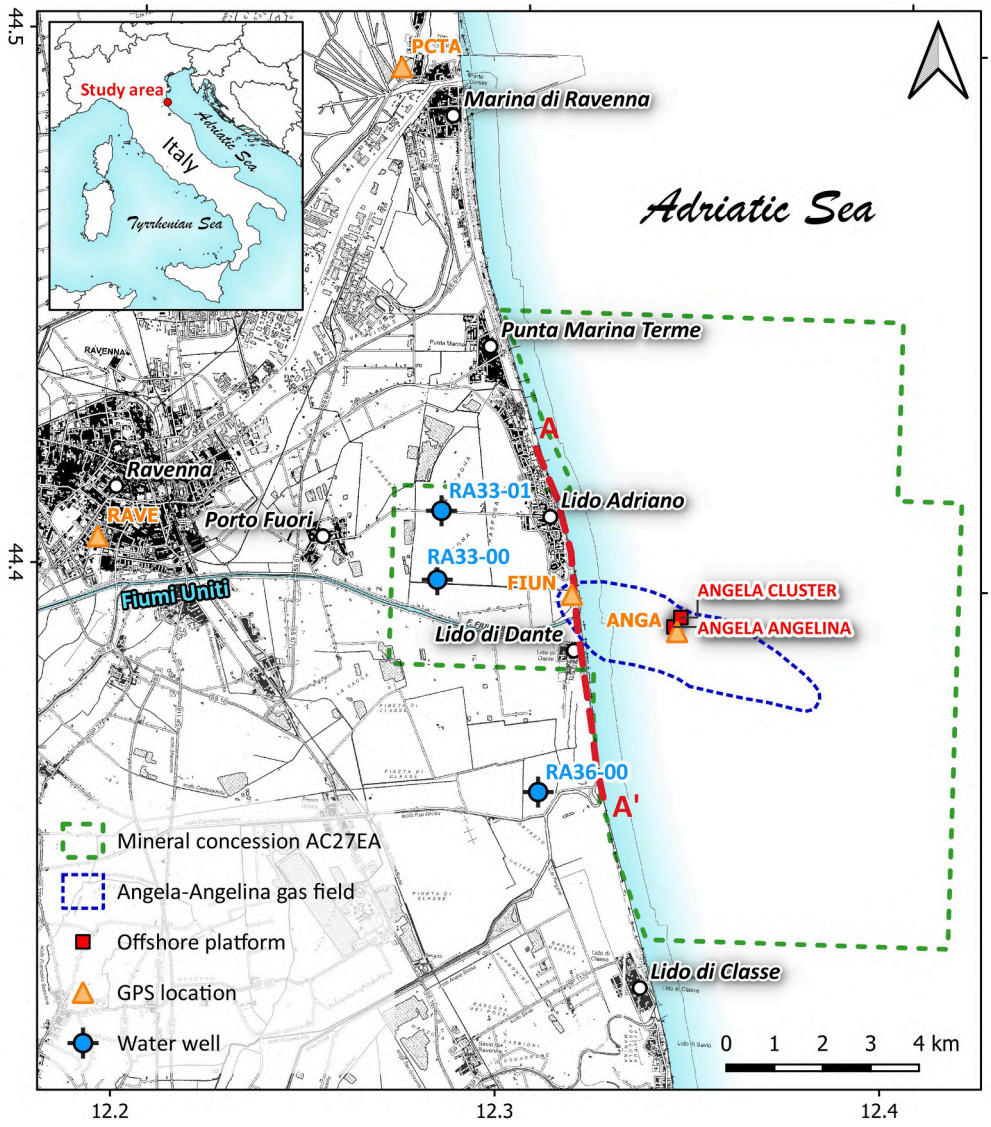

Fig. 1. Sketch of the study area. The dashed green line indicates the extent of the mineral concession area, the red squares locate the offshore platforms, the blue circles indicate the location of available water-wells, the orange triangles represent the GPS stations and the dashed blue curve indicates the projection at the surface of the reservoir.

2002; Teatini et al., 2005; Teatini et al., 2006) also including a mineral concession area directly overlaid by the shoreline extending from Lido Adriano to Lido di Dante villages (Fig. 1).

2. Data and methods

2.1. InSAR data

The InSAR dataset consists of C-and X-band SAR images acquired by Envisat, Sentinel-1 (S1) and Cosmo-SkyMed (CSK) missions of the European Space Agency (ESA) along both ascending and descending orbits.

The C-band Envisat dataset includes 101 images spanning from december 2002 to september 2010 whereas the C-band S1 dataset consists of 227 images covering the March 2015 - July 2018 time span. Both S1 ascending and descending data are acquired with an incidence angle of about 39°, which is quite higher than that of Envisat and CSK sensors (~27°), thus allowing a better sensitivity in the East-West (EW) displacement component.

The X-band CSK dataset consists of 216 SAR images from september 2011 to december 2017 thus partially filling the temporal gap of more than 4 years between Envisat and S1 missions time windows. Moreover, the high spatial resolution of X-band data (~3 m of pixel spacing) allows to preserve more details than C-band data, including the deformation affecting the offshore platform, whose dimensions are about 50x25m.

Additionally, the Italian Energy Company Eni S.p.A. made available an InSAR dataset based on Radarsat-2 SAR images in the framework of the "CLYPEA: Innovation network for future energy" Program, as part of the "subsoil deformations" Project (Antoncecchi et al., 2018, 2019). This dataset consists of InSAR displacement maps and relative time series acquired from the C-band sensor of the Canadian Space Agency (CSA) between 2004 and 2018 and can be exploited as further validation of the reliability of the data processing performed in this study (Supplementary Material).

InSAR analysis was performed by adopting the Multi-Temporal Interferometric Point Target Analysis (IPTA) approach, in the framework of GAMMA software (Werner et al., 2003). Concerning the onshore data processing, we applied multilook factors such to reduce the speckle noise characterizing SAR images and retrieve a pixel spacing of about 90 m, i.e., the same size of the Digital Elevation Model (DEM) provided by Shuttle Radar Topography Mission (SRTM) (https://www2.jpl.nasa.gov/srtm/), exploited for removing the topographic contribution in differential interferometric phase.

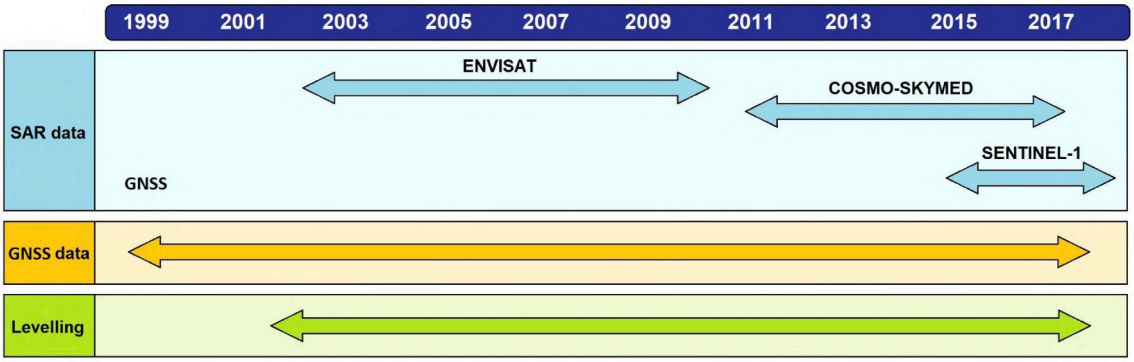

Fig. 2. Chart of the available datasets exploited in this work.

Instead, for the offshore processing with CSK data, we first worked with resolution consistent with the dimensions of the platform (~30 m) to evaluate its deformation with respect to the same inland reference point used for the onshore analysis.

Then, we exploited the full-resolution data (~3m) to obtain as many InSAR point targets as possible on the platform and detect any differential deformations among different parts of it.

2.2. GNSS data

The GNSS measurements were retrieved from continuous stations belonging to public institutions and private companies (Serpelloni et al., 2013; Devoti et al., 2017), integrated by additional data from stations installed on offshore platforms and provided by Eni S.p.A. (Palano et al., 2020). The dataset presented here is part of a continental-scale geodetic solution of more than 3000 continuous GNSS stations operating in the Euro-Mediterranean region (Serpelloni et al., 2013; Devoti et al., 2017). The time span covered by the GNSS acquisitions ranges from 1999 to the end of 2017 (Fig. 2).

Following the procedure described in Serpelloni et al. (2018), the daily GNSS raw data were processed by the GAMIT/GLOBK software (Herring et al., 2018). In particular, we analysed the observations recorded by the GNSS stations of a sub-network that includes the Eni stations plus other permanent GNSS ones, realising a weakly constrained network solution (positions, orbits, etc.). The loosely constrained solutions obtained from the GAMIT processing were combined with the global solution of the IGS network (available at ftp://everest.mit.edu/pub/MIT_GLL/) and aligned to the global IGb08 reference frame. Further technical details are reported in Palano et al. (2020) and Serpelloni et al. (2018). The final horizontal position time series were rotated with respect to an Adria-fixed reference frame using the rotation pole from Serpelloni et al. (2016), in order to highlight possible differential movements among the GNSS stations located in the study area.

We performed the GNSS displacement time series analysis estimating a constant velocity term, along with annual and semi-annual seasonal components and, if required, offsets at specific epochs representing equipment changes, coseismic motions, or other displacements of the antenna phase centres. Velocity uncertainties were estimated by using the maximum likelihood estimation technique implemented in the CATS software (Williams, 2008), and considering the presence of white noise and Flicker noise in the GNSS time-series. We removed outliers taking into account a post-fit time series Root-Mean-Square (RMS) criterion,

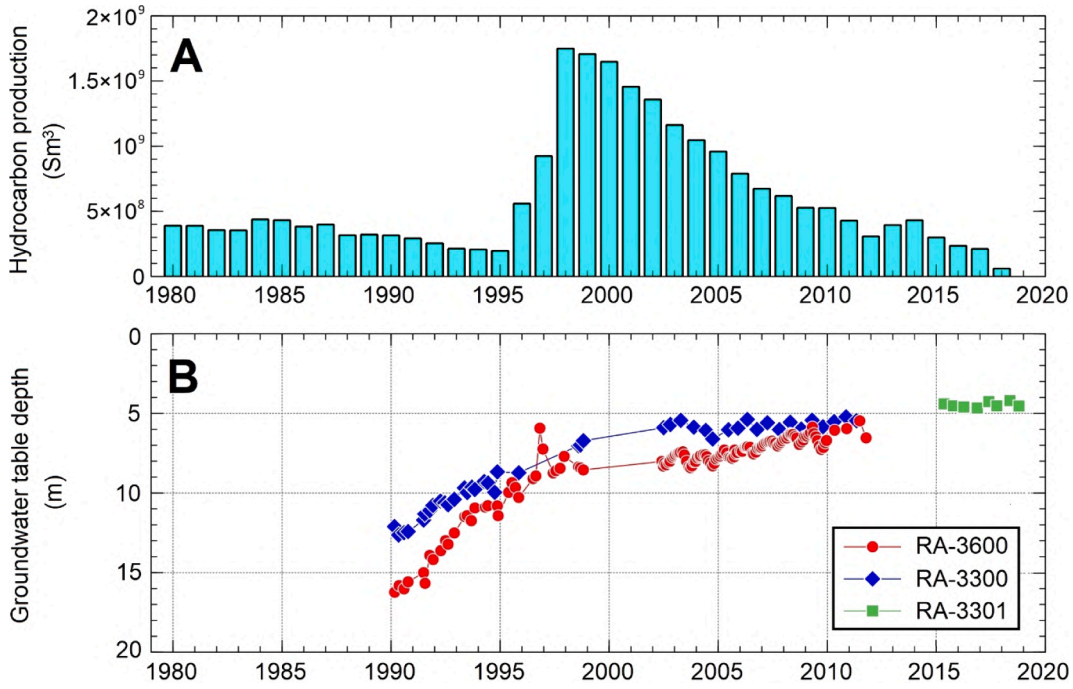

Fig. 3. (A) Annual hydrocarbon production at the gas field. (B) Depth of the groundwater table with respect to the ground level measured at water wells RA33-00, RA33-01 and RA3600, located near the Lido di Dante area and reported in Fig. 1.

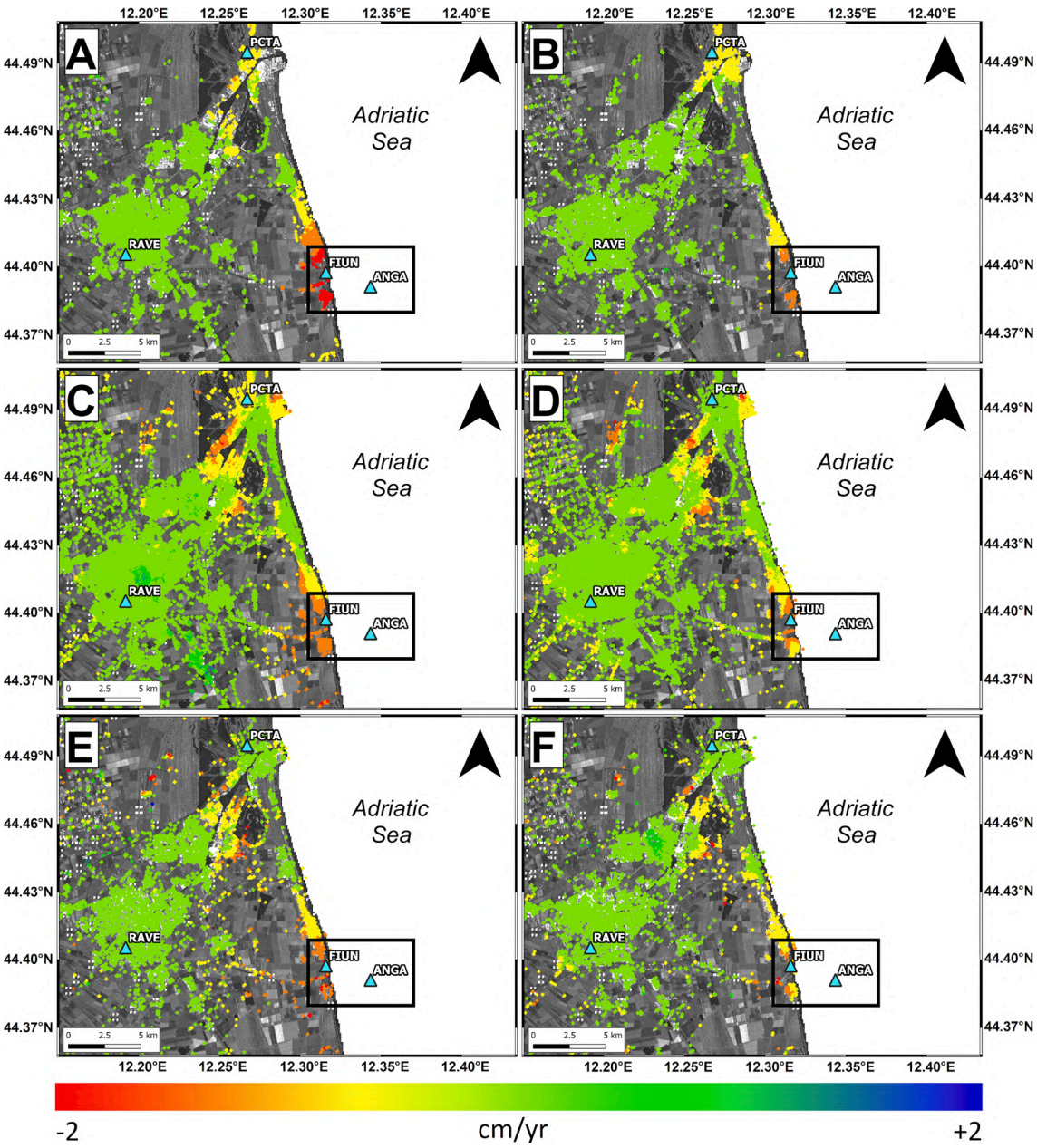

Fig. 4. InSAR LoS velocity maps retrieved by Envisat Ascending (A) and Descending (B) (2002–2010), CSK Ascending (C) and Descending (D) (2011–2017), S1 Ascending (E) and Descending (F) (2015–2018) data. The light-blue triangles show the location of the GNSS stations. The background image has been obtained by a CSK SAR intensity image. The black rectangle indicates the Area of Interest with the Lido di Dante area and the offshore platform. The position of RAVE GNSS station is used as reference point for InSAR analysis. (For interpretation of the references to colour in this figure legend, the reader is referred to the web version of this article.)

according to which we discard GNSS epochs whose position values are larger than three times the post-fit Weighted-RMS (WRMS). In this analysis, from the entire analysed dataset we extracted solutions only for four GNSS stations which are characterized by an observation period longer than 10 years and covering our small area of study, therefore allowing for a good spatial and temporal overlap with other geodetic techniques.

2.3. Leveling data

The Leveling dataset were provided by Eni S.p.A. in the framework of "CLYPEA" project and includes the lines across the study area for a total amount of 147 benchmarks. We selected the measurements carried out since 2002 because the elevation values are more reliable being certified by the provider and the measurements overlap with the InSAR time series described above (Fig. 2).

The considered Leveling campaigns took place in 2002, 2003, 2004, 2005, 2007, 2009, 2011, 2014, and 2017. This dense sampling allowed us to calculate mean ground velocities by linear regression analysis and to compare them with InSAR and GNSS measurements. All velocities were scaled with respect to a reference benchmark located in the city of Ravenna, whose displacement was imposed to be zero.

2.4. Ancillary data

Available ancillary data consist of hydrocarbon annual production rate and groundwater table depths registered at some wells located over the study area (Fig. 1). The annual gas production (Fig. 3a) from 1980

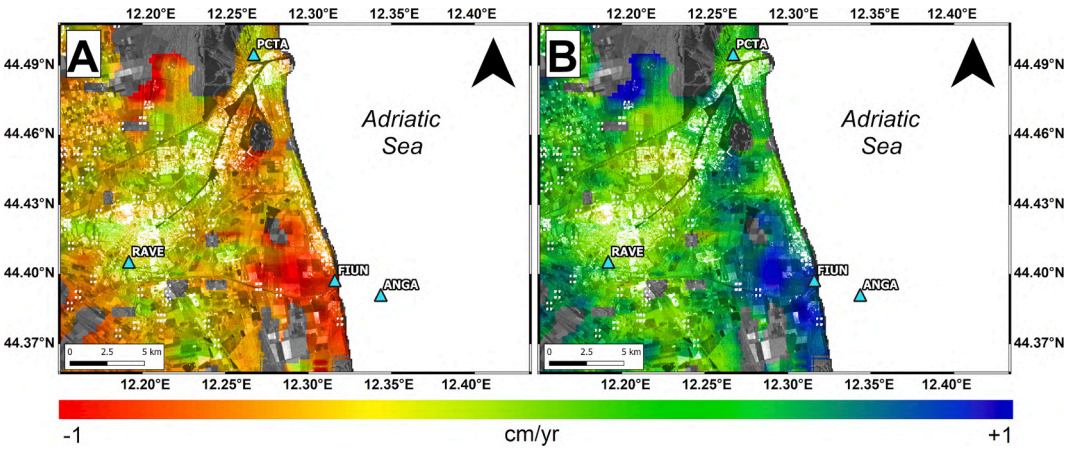

Fig. 5. S1 LoS displacement rates decomposed in UP (A) and EW (B) components (2015–2018). The light-blue triangles represent the GNSS stations. The background image has been obtained by a CSK SAR intensity image. The position of RAVE GNSS station is used as reference point for InSAR analysis. (For interpretation of the references to colour in this figure legend, the reader is referred to the web version of this article.)

until early 2018 (https://unmig.mise.gov.it/index.php/it/) shows peak between 1997 and 1999 corresponding to the start of production from 14 wells perforated at the offshore platform (Fig. 1). After the early 2000 s, the extraction activity gradually decreased, reaching annual production rates similar to those prior to 1995.

Concerning the hydrogeological data, depth of groundwater level of the multi-layered surficial aquifer is measured at three water-wells used for irrigation purposes, namely RA33-00, RA33-01, RA36-00 (Fig. 1), and made available by the Regional Agency for Prevention, Environment and Energy (ARPAE) of Emilia-Romagna (Italy). These data (Fig. 3b) show that the groundwater table depth progressively decreased from 1990 to 2019 with a rate of ~ 0.8 m/yr during 1990–1999 and of 0.1–0.3 m/yr during 1999–2012, while no significant depth variations can be observed since 2015.

3. Results

3.1. Onshore and offshore InSAR displacements

Regarding the onshore processing, ascending and descending Envisat (Fig. 4, A-B), CSK (Fig. 4, C-D) and S1 (Fig. 4, D-E) Line-of-Sight (LoS) InSAR velocity maps show a clear deformation pattern located along the coastline in the proximity of Lido di Dante and Fiumi Uniti villages, with rates up to about −2 cm/yr. Deformation rates decrease over time, from

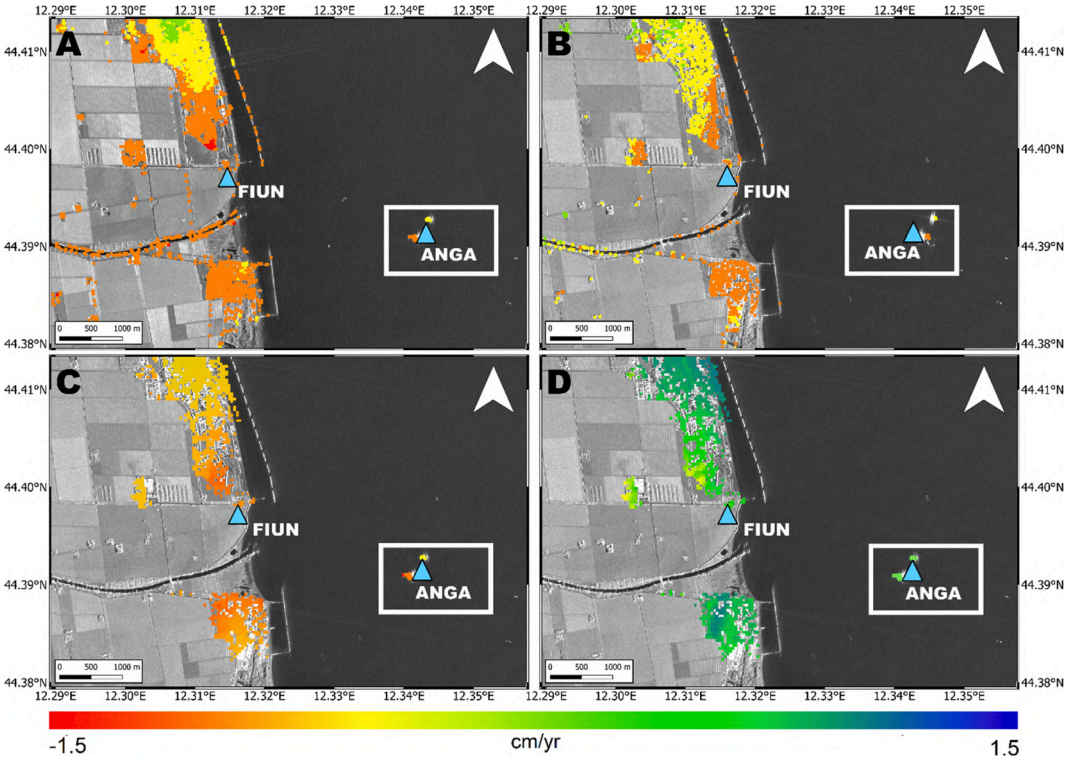

Fig. 6. LoS velocity maps retrieved by CSK InSAR data at medium resolution along ascending (A) and descending (B) orbit; Vertical (C) and horizontal (EW) displacement rates (D). The light blue triangles represent the onshore (FIUN) and offshore (ANGA) GNSS stations. The background image has been obtained by a CSK SAR intensity image. The white rectangle indicates the position of the offshore platform. (For interpretation of the references to colour in this figure legend, the reader is referred to the web version of this article.)

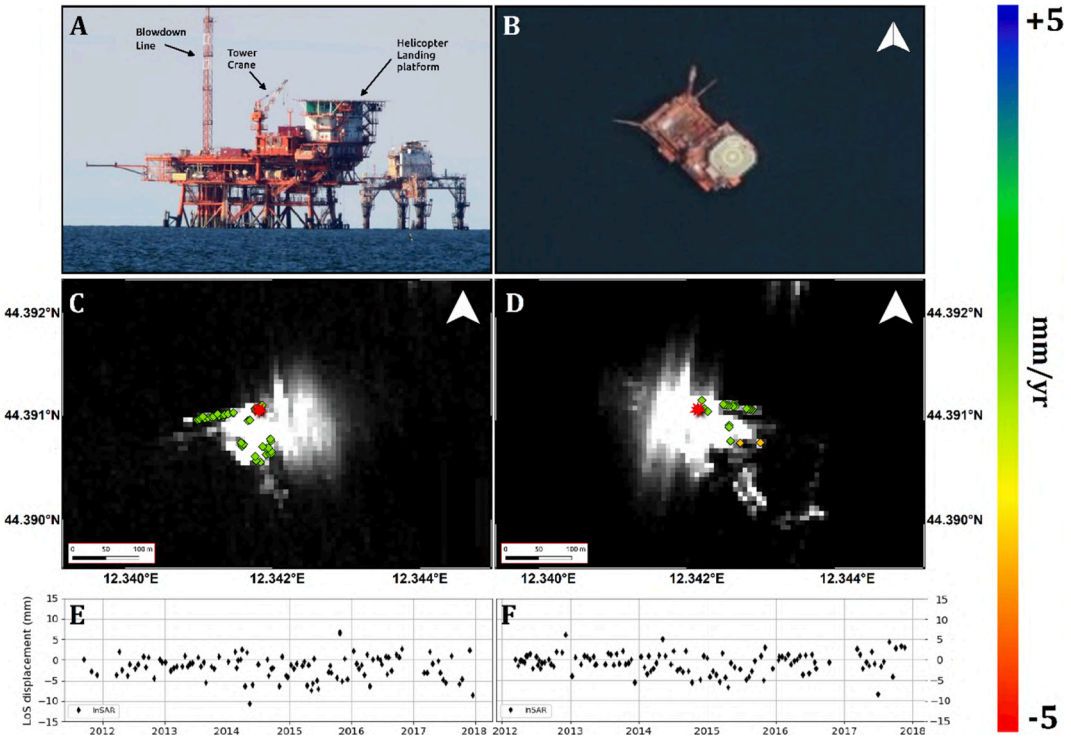

Fig. 7. Focus on the offshore platform: picture taken from the Bevano mouth (source: https://www.ilrestodelcarlino.it/ravenna/cronaca/eni-de-pascale-1.3252246) (A) and aerial view by Esri satellite map available in QGIS software (http://qgis.osgeo.org) (B). CSK InSAR LoS deformation rate for ascending (C) and descending (D) data. The red star represents the reference point used to evaluate differential movements of the platform. Ascending (E) and descending (F) InSAR CSK time series retrieved from two points on the platform. (For interpretation of the references to colour in this figure legend, the reader is referred to the web version of this article.)

about −2/-1.5 cm/yr in the Envisat maps 2003–2010 to −0.5/-1 cm/yr in the S1 ones (2015–2018).

Combining ascending and descending data, vertical (UP) and East-West (EW) velocity components can be calculated (Dalla Via et al., 2012; Fuhrmann and Garthwaite, 2019), being the SAR sensors almost blind to the NS displacements. Such operation preliminarily requires the interpolation of LoS ascending and descending velocities to fill any gaps between the outcomes from each track. This could produce some interpolation errors especially in areas where the data are missing and then it should be seen as a qualitative estimation. Anyway, the results of such analysis are shown in Fig. 5 for S1 data that are the most sensitive to the EW component due to the larger incidence angle of about 39°. The UP and EW displacement components are comparable in both spatial extent and magnitude, indicating that Lido di Dante experienced both ground subsidence (Fig. 5a) and eastward movements (positive values in Fig. 5b) during the 2015–2018 period.

For the offshore SAR analysis, we focus on the platform present in the area (Fig. 1). We evaluated the mean deformation of the entire platform and constrained possible deformation gradients along different sides of the platform itself.

The first analysis identifies deformation rates of the whole platform peaking at about −1 cm/yr (Fig. 6). We retrieve similar values on the platform for both ascending and descending data (Fig. 6, panels A-B) suggesting that the retrieved deformation pattern is purely vertical, while the EW component can be considered negligible, as shown by the decomposition of the motion in vertical and horizontal components (Fig. 6, panels C-D).

For the small-scale analysis we consider a very local processing, focusing only on the platform, depicted in Fig. 7, A-B. The latter, in a SAR image, appears as a very coherent and bright object surrounded by an incoherent and dark sea (Fig. 7, C-D). One of the point scatterers on the platform is used as a reference point, in order to evaluate any relative movements (red star in Fig. 7, C-D). No significant velocity gradients between different parts of the platform can be inferred, meaning that differential movements detectable within the limit of accuracy of the technique are not taking place. In panels E-F of Fig. 7, we report the displacement time series for two targets on the helicopter-landing platform. The descending orbit data shows two point scatterers with higher displacement rates (about −2 mm/yr) corresponding to the drilling tower (orange in Fig. 7, panel D). Being a relatively small signal, we are not completely confident about that since it is observed only along one track. Moreover, the different platform parts such as the tower crane and the blowdown line are characterised by different heights, thus they could lead to possible artefacts, multipath effects and “topographic-like” errors (Fig. 7, panel A).

3.2. GNSS and Leveling displacements

The GNSS velocities are shown in Fig. 8. The horizontal velocities are referred to the Adria-fixed reference frame, which assumes the central part of the Po Plain, the Northern sector of the Adriatic Sea and the Istria peninsula as a stable rigid block (e.g., Devoti et al., 2008; Devoti et al., 2011; D’Agostino et al., 2008; Serpelloni et al., 2016). The measured horizontal velocities (grey arrows in Fig. 8 A) span from 1 to 2 mm/yr to more than 7 mm/yr. In this specific reference frame, the expected tectonic velocities are in the range of 1–2 mm/yr along the NE-SW direction (e.g., Serpelloni et al., 2016; Devoti et al., 2017; Palano et al., 2020, Pezzo et al., 2020), as represented by the RAVE station. Instead, for the other GNSS sites higher horizontal velocities can be ascribed to other natural or anthropogenic deformation sources. GNSS vertical velocities (coloured circles in Fig. 8, panel A) indicate subsidence rates ranging from 3 mm/yr up to 17 mm/yr, where the highest values are recorded in correspondence of Fiumi Uniti (FIUN station) and at the offshore platform (ANGA station).

In order to cross-validate our results, we refer the GNSS displacement time series and velocities to the same reference point of InSAR and Leveling displacements, i.e., the RAVE station. Although the velocity of this site is not null in the Adria-fixed reference frame (about 3 mm/yr

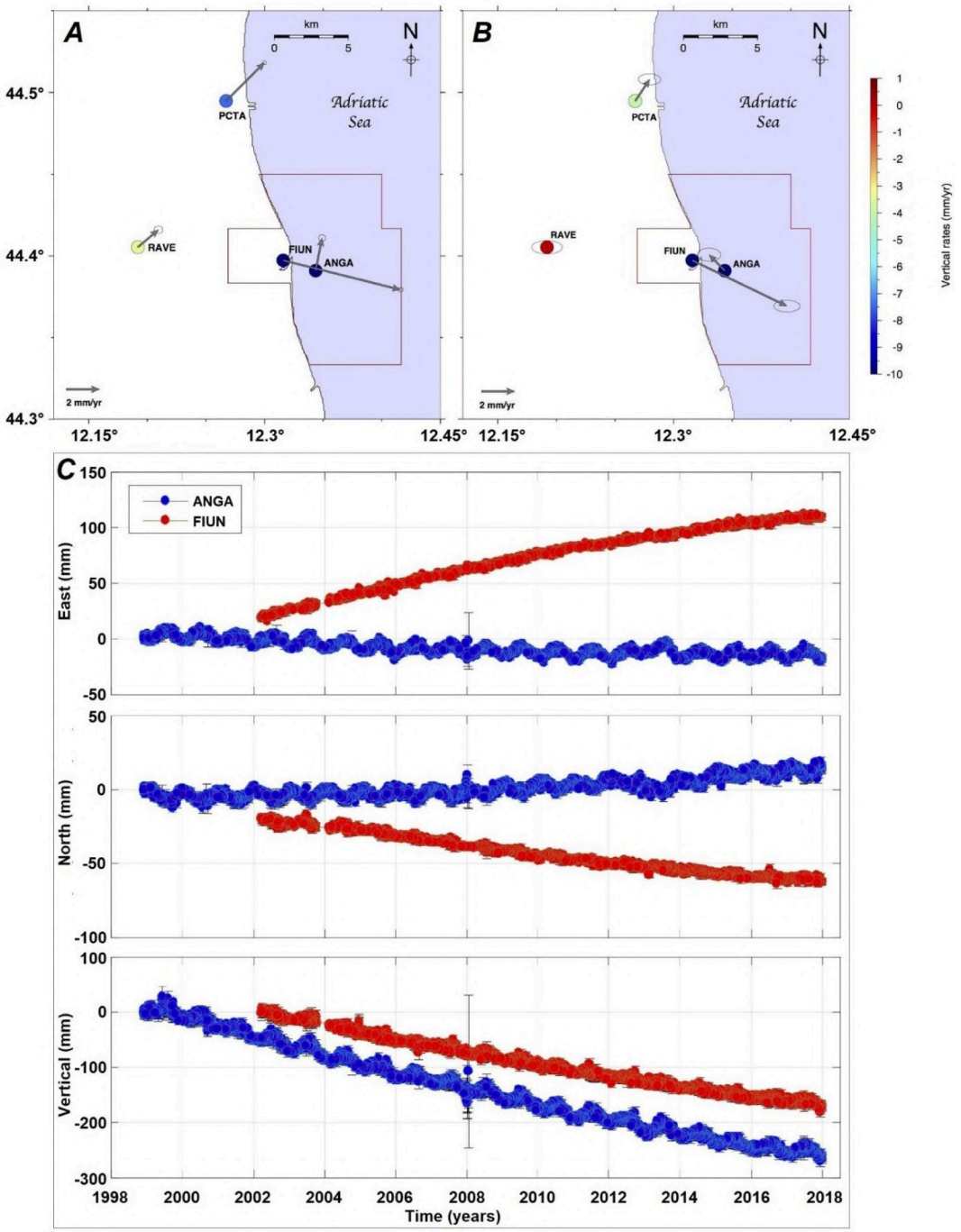

Fig. 8. A) Horizontal (grey arrows) and vertical (coloured circles) GNSS velocities with respect to a local (Adria-fixed) reference frame (see the main text for details), and with respect to RAVE station (Panel B). The red polygon indicates the mineral concession "AC.27.EA". C) Time series of the three displacement components of ANGA and FIUN stations, referred to RAVE; the vertical bars are the 1 error associated with each daily position. (For interpretation of the references to colour in this figure legend, the reader is referred to the web version of this article.)

and 2 mm/yr for the vertical and horizontal component, respectively), they appear considerably lower than the PCTA, FIUN and ANGA ones. Fig. 8B shows the horizontal and vertical velocities with respect to RAVE, highlighting the strong localized subsidence occurring at more than 1 cm/yr for both FIUN and ANGA stations. Moreover, we observe the mostly-eastward horizontal displacement rate (~6 mm/yr) of the FIUN station, also highlighted by the displacement time series in panel C of Fig. 8. Conversely, ANGA station time series (Fig. 8 C) mainly shows a strong vertical component, whereas both NS and EW horizontal ones are much less significant. These results further corroborate that Lido di Dante area is characterised by local ground subsidence and eastward displacements, in agreement with InSAR analysis.

Finally, we consider the vertical displacement rates from Leveling data covering the 2002–2017 time interval (Fig. 9). Such velocities evidence an increasing at Lido di Dante and Fiumi Uniti villages, where the rates span from about −1 cm/yr to −1.5 cm/yr whereas are close to zero moving away up to the city of Ravenna, where the RAVE station is located.

3.3. Geodetic data cross-validation

In order to validate the outcomes retrieved by the analysis of InSAR,

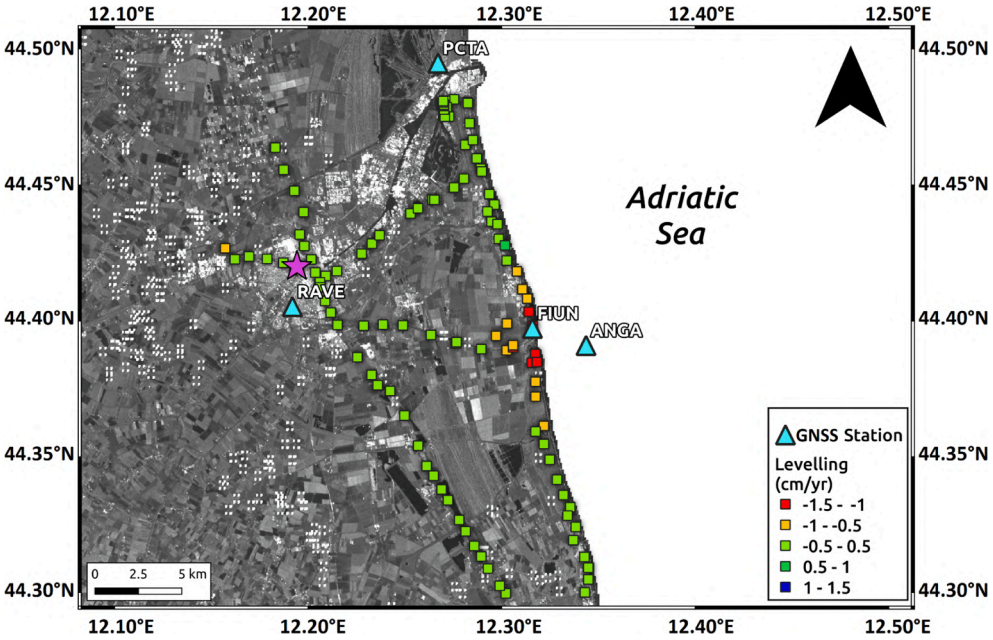

Fig. 9. Vertical deformation velocities detected by Leveling surveys. The fuchsia star is the reference point. The blue triangles represent the GNSS stations owned by a local public authority (RAVE) and Eni S.p.A. (PCTA, FIUN and ANGA). The background image has been obtained by a CSK SAR intensity image. (For interpretation of the references to colour in this figure legend, the reader is referred to the web version of this article.)

GNSS and Leveling data, we compare the displacement time series retrieved by these different techniques by choosing the same reference point in the proximity of RAVE GNSS station. In this way, all results are representative of displacements relative to the same point in space.

The selection of RAVE station as reference is motivated by the following reasons: i) it is covered by all SAR frames; ii) it experiences high coherence of SAR signal, as usually happen in urban areas, allowing to minimize the temporal decorrelation effects; iii) it is close enough to the AOI such to avoid unwrapping errors during InSAR processing and ensure reliable measurements; iv) in the same time it is far enough (about 10 km) from the AOI to rule out the influence of the same deformation phenomenon.

The choice of the reference system has to be taken into account in the data interpretation, since it leads to the minimization of the contribution due to the natural compaction phenomenon, which is roughly constant along the entire Ravenna coastal region and estimated to be about 2.5–5 mm/yr by Gambolati and Teatini (1998) and Mantovani et al. (2013).

The comparison between InSAR and LoS-projected GNSS displacement time series for FIUN and PCTA stations is shown in Fig. 10. Indeed, when possible InSAR and GNSS data comparison should be performed along each satellite LoS since i) the InSAR data are almost insensitive to NS displacements; ii) both SAR orbits are required in order to compute EW and UP components and it may introduce additional errors due to the misalignments between ascending and descending point scatterers. The results are consistent with each other and they clearly show a deceleration in time of the phenomenon. Indeed, considering the ascending data in Fiumi Uniti (FIUN station), the displacement estimated by the Envisat and LoS-projected GNSS data from 2002 to 2010 is about 10 cm (Fig. 10, Fiumi Uniti, panel A), while it is about half and a quarter for LoS-projected GNSS and CSK and S1 InSAR data in the time interval 2011–2017 (Fig. 10, Fiumi Uniti, panel C) and 2015–2018 (Fig. 10, Fiumi Uniti, panel E), respectively.

To cross-validate the Leveling data with InSAR and GNSS datasets, we need to compare the vertical component since it is the only one constrained by such technique. The vertical component from different SAR sensors is retrieved by combining ascending and descending data, as previously mentioned. Being independent by the geometry of view of each satellite, the vertical time series from the three SAR datasets can be connected in time thus offering a synoptic view of the subsidence phenomena occurring in the study area from 2002 to 2018. Then, in the case of Fiumi Uniti, which is the only site covered by InSAR, GNSS and Leveling data, we additionally performed a cross-validation by comparing the vertical displacement time series retrieved by all the data sources. The same, but only with InSAR and Leveling data, has been done in Lido di Dante area, where a cumulated deformation of approximately 16 cm in 16 years took place (Fig. 11). Also in this case, the agreement between trends is encouraging, supporting the reliability of the results. The deceleration of the subsidence is particularly evident in Lido di Dante area where we observe about 10 cm of displacement from 2004 to 2011 and about 5–6 cm in the following 7 years (Fig. 11B).

Fig. 12 shows an additional analysis performed by comparing the vertical velocity from Leveling and InSAR data along the coastline. In this case, we exploit only Envisat SAR data since they ensure the best temporal overlapping with Leveling campaigns. Results are consistent with each other, showing similar trends from Lido Adriano to Bevano river mouth and confirming a maximum displacement rate in the area of Lido Di Dante and Fiumi Uniti. InSAR and Leveling outcomes are also in agreement with the vertical component of FIUN station, shown in the coastline profile.

Regarding the offshore cross-validation, we compare the LoS-projected GNSS measurements of ANGA station with the InSAR time series retrieved by the medium resolution CSK data processing (Fig. 13). The results show a similar trend with subsidence values up to 6 cm detected by both data sources from 2012 to 2017. We also observe significant seasonal signals, probably due to the thermal expansion/contraction of the platform, which is constrained in agreement by the two datasets.

In order to provide a quantitative evaluation of the cross-validation procedure, we finally estimated the linear correlation coefficient between the different time-series in the Fiumi Uniti, Lido di Dante and Porto Corsini areas and at the offshore platform (Table 1). We find very high correlation values ranging from 0.8 to 0.95 in most cases, with slightly lower values in the Porto Corsini area.

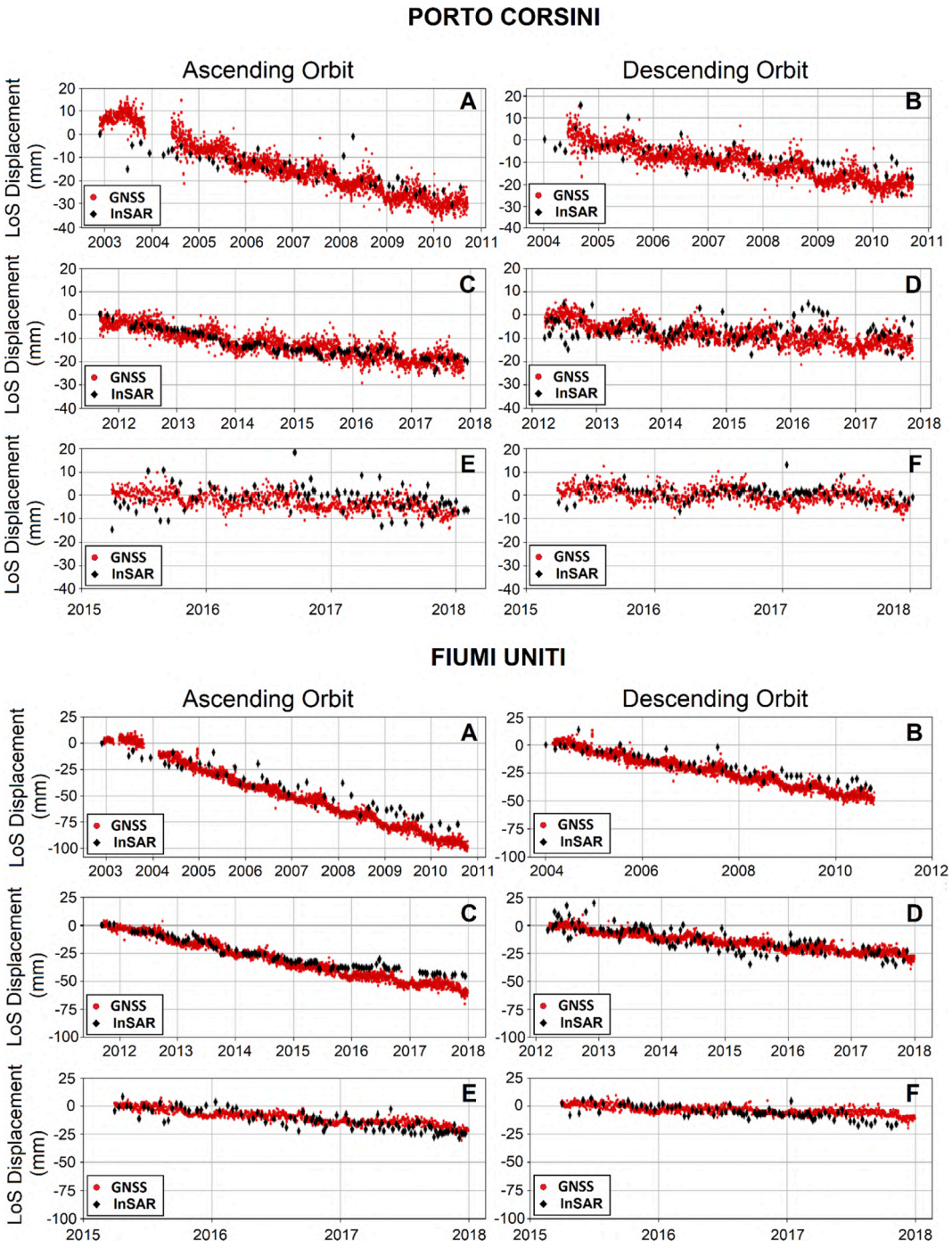

Fig. 10. Los projected GNSS-InSAR time series comparison in Porto Corsini (PCTA station) and Fiumi Uniti (FIUN station) areas considering Envisat ascending (A) and descending (B), CSK ascending (C) and descending (D) and S1 ascending and descending SAR data.

4. Discussion

In this paper we analysed about 20 years of geodetic data related to the Upper Adriatic Sea coasts (Italy) where different phenomena contribute to the ground subsidence. The synergistic use of different techniques allows to obtain a synoptic view of the observed ground displacement field and its changes through time. Indeed, the outcomes from InSAR, GNSS and Leveling data are fully complementary, being able to constrain the deformation field with dense temporal sampling, large spatial coverage and millimetric accuracy. However, some errors may occur due to data processing inaccuracies, atmospheric artefacts, wear and lacking maintenance of the instruments or sensor random noise. Concerning InSAR data, typical errors on a single measurement are in the order of about 5 mm (Casu et al., 2006) whereas GNSS daily displacements show uncertainties of about 1 mm and 3 mm for the horizontal (both North-South and East-West) and vertical components, respectively. Instead, the accuracy of Leveling data strictly depends on the considered network of benchmarks and the distance from the reference. Indeed, for a given benchmark, the maximum accepted uncertainty in mm on the measured altitude values can be approximately expressed as $2\sqrt{L}$ where L is the distance in Km from the reference. However, in the considered case study, Eni S.p.A., i.e. the owner of Leveling data, did not provide the uncertainty of the measurements. In addition, the strategy for the choice of reference is different for some

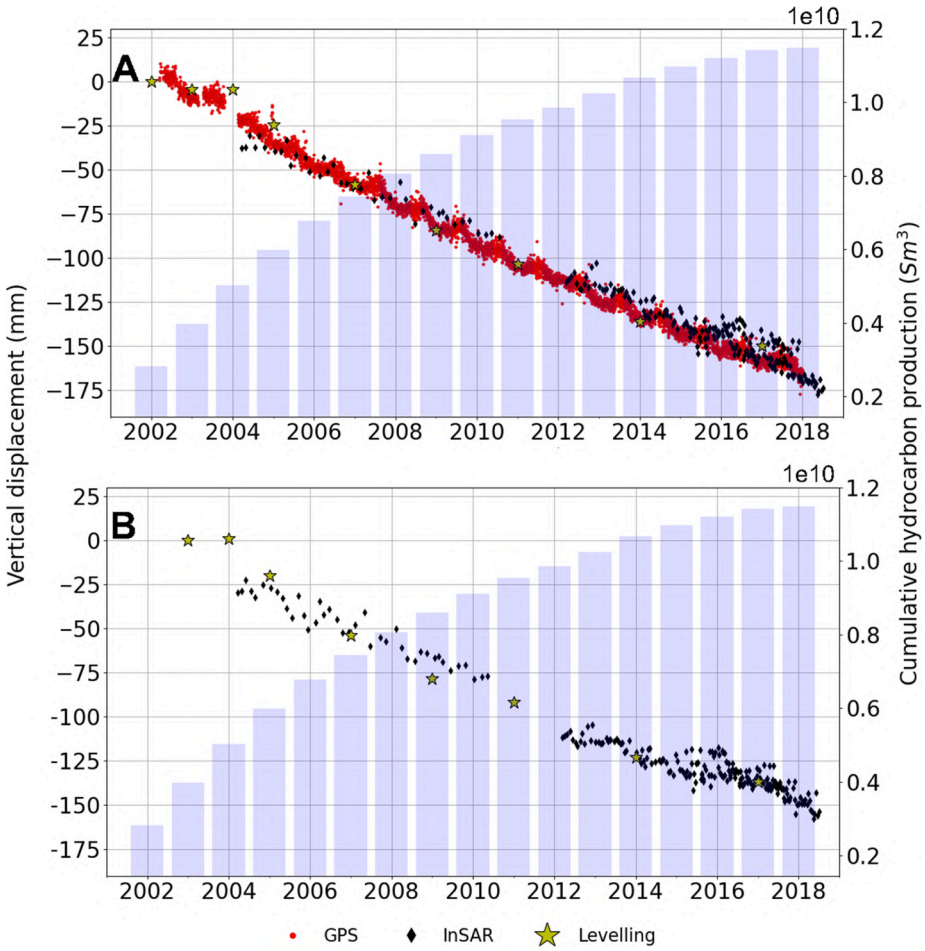

Fig. 11. Vertical displacement time series comparison in Fiumi Uniti (A) and Lido di Dante (B) areas. Both panels also show the cumulative gas production of the gas field from 2002 to 2018.

campaigns thus preventing the estimation of an absolute maximum value for the uncertainty. The only value we can estimate is the relative uncertainty when we move the reference in Ravenna city which is approximately equal to 6 mm for the entire AOI.

A way to be confident with the measurements is to validate all the available outcomes from different techniques by a cross-comparison procedure. Such approach is not straightforward due to several inhomogeneities caused by different geometries, acquisition modes and reference systems that have to be first analysed and addressed.

The choice to project the GNSS measurements into the SAR LoS and not *vice versa* should be done since InSAR data can be decomposed into UP and EW components while they are almost insensitive to the NS, thus making the cross-validation procedure incomplete.

Moreover, sharing the same reference system is essential to rigorously comparing different data. Indeed, the reference systems usually used for the GNSS networks aim at investigating regional tectonic trends, whereas InSAR data estimate relative motion in space and time with respect to a specific point target in the SAR frame. On the other hand, in the Leveling technique the vertical component is referred to a fixed site but the errors increase with the distance.

To properly study local deformation fields, it is strongly suggested to adopt a simplified reference frame given by a common reference (GNSS or Leveling benchmarks) inside the SAR frame as reference point. This allows to minimize any error propagation and isolate as much as possible the source of deformation.

Data analysed in this study encompasses a mineral concession area along the Upper Adriatic Sea coasts highlighting different characteristics of the detected displacement field: i) the onshore deformation peaks in the proximity of Fiumi Uniti and Lido di Dante villages with cumulative displacement values of about 16–17 cm from 2002 to 2018; ii) it is the combination of both vertical (subsidence) and eastward movement; iii) the offshore deformation mostly consists of vertical displacements; iv) both onshore and offshore deformation are decelerating in the last years.

After the cross-validation procedure, we retrieve high correlation values between the different techniques, thus demonstrating the reliability of the measurements. InSAR and GNSS data for the sites inside the concession area show consistent outcomes in terms of LoS-projected measurements, with correlation values ranging from 0.84 to 0.95, whereas the vertical component compared in Fiumi Uniti has a correlation of 0.73. Such difference is likely due to the significant horizontal component, which is instead taken into account in LoS measurements and the possible error propagation when decomposing InSAR LoS displacements. Where available (Fiumi Uniti and Lido di Dante), Leveling data show a good agreement with both GNSS and InSAR measurements, despite the limited number of Leveling campaigns.

Lower correlations between InSAR and LoS-projected GNSS measurements are found in Porto Corsini area (PCTA station), about 10 km north of the AOI, especially considering S1 data, with values of 0.55 and 0.75 for ascending and descending data. This is likely due to the lack of a clear deformation trend in the last years (Fig. 10, *Porto Corsini* E-F), thus correlating some random noise of the two techniques.

Then, our procedure provides an unprecedented 20-years window reliable estimation of land subsidence, which can support quantitative assessment and modelling of the different concurrent phenomena. Here, discriminating between the different origins of the observed pattern is beyond the scope of this manuscript, but a qualitative interpretation can

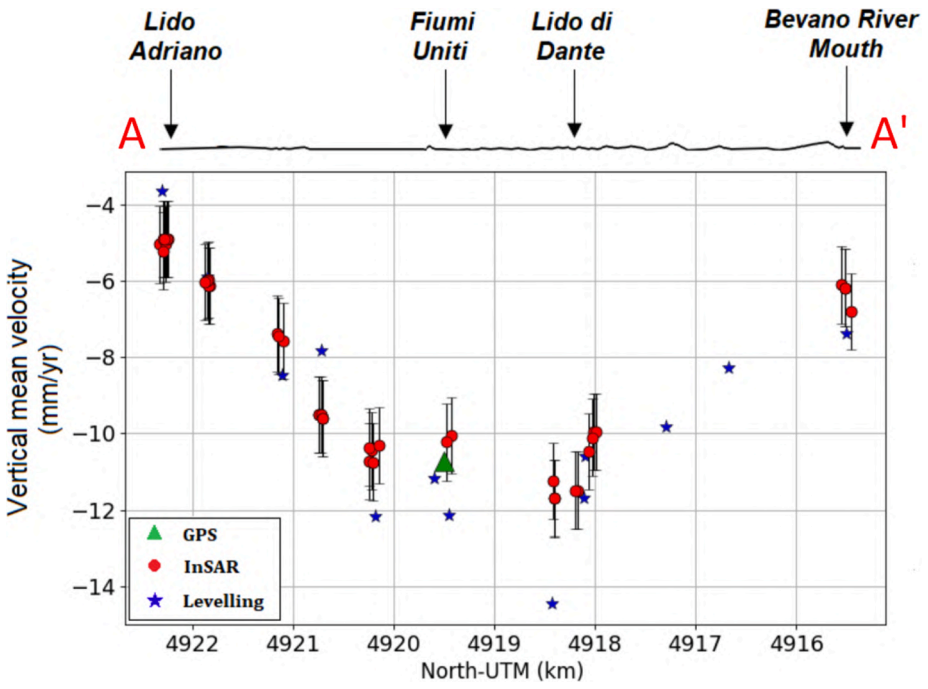

Fig. 12. InSAR-Leveling vertical displacement rate comparison during 2002–2010 considering Envisat SAR data. The comparison Is performed with the benchmarks located along the coastline indicated as AA' dashed red line in Fig. 1. (For interpretation of the references to colour in this figure legend, the reader is referred to the web version of this article.)

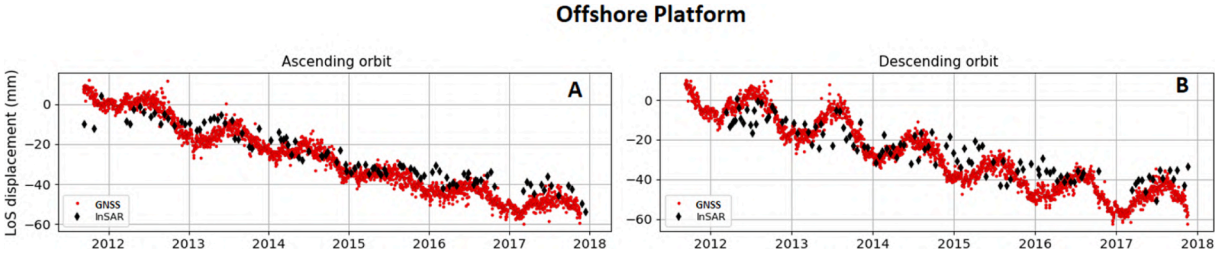

Fig. 13. Los projected GNSS-InSAR time series comparison at the offshore platform considering CSK medium-resolution SAR data.

Table 1
Summary of the correlation coefficients between the different data sources.

	Vertical component	*LoS Ascending Envisat*	*LoS Descending Envisat*	*LoS Ascending CSK*	*LoS Descending CSK*	*LoS Ascending S1*	*LoS Descending S1*
GNSS-InSAR	0.73	0.94	0.91	0.84	0.86	0.85	0.88
GNSS-Leveling	0.92	–	–	–	–	–	–
InSAR-Leveling	0.89	–	–	–	–	–	–
GNSS-InSAR		–	–	0.92	0.86	–	–
InSAR-Leveling	0.98		–	–	–	–	–
GNSS-InSAR	–	0.88	0.74	0.95	0.73	0.55	0.75

be provided by combining the retrieved results with other available information. Indeed, the regional tectonic component, which is quite constant over the investigated area (Gambolati and Teatini, 1998, Pezzo et al., 2020) was significantly minimized by setting the reference system in Ravenna city. Another important contribution comes from the consolidation process of the Holocene sediments of the shallow coastal aquifer which has been estimated to account for 10–20% of the observed land subsidence (Antonellini et al., 2019). Ancillary data (i.e., gas production and groundwater withdrawal) provide additional information about causes and evolution over time of the phenomenon. The horizontal displacement trends of both InSAR and GNSS (in particular the FIUN station) are directed towards the centre of the gas field, therefore suggesting a deformation component due to the reservoir depletion. On the other hand, the contribution to the ground subsidence caused by the overexploitation of the surficial multi layered aquifers could be less important since the depth of the groundwater table monitored at some relevant wells surrounding the study area (Fig. 3, panel B) shows a decreasing trend from 1990 to 2019 meaning that no significant water pumping activities have been recently performed in the area. This is consistent with previous studies showing low subsidence values induced by aquifer exploitation activities since 2001 (Gonella et al., 1998; Teatini et al., 2006), in contrast with subsidence rates up to 60 mm/yr

observed for the most of the Ravenna Municipality during the 1972–1977 period (Teatini et al., 2005).

5. Conclusions

We applied an approach based on geodetic data cross-validation to provide a reliable and quantitative assessment in space and time of the land subsidence affecting the Upper Adriatic Sea coastline. We found a good correlation of the results obtained from InSAR, GNSS and Leveling techniques for both onshore sites and offshore sites. Our results highlight a subsidence pattern up to −1/-1.5 cm/yr in the proximity of the coastline, close to Lido di Dante and Fiumi Uniti villages, and at the offshore platform. Corresponding time series reveal a decreasing pattern from 2002 up to the present days, setting at values lower than −1 cm/yr. Starting from the quantitative assessment of the deformation carried out in this work, the discrimination and modelling of the different contributions will be matter of further analysis.

Declaration of Competing Interest

The authors declare that they have no known competing financial interests or personal relationships that could have appeared to influence the work reported in this paper.

Acknowledgements

This research was financed by the Italian Ecologic Transition Ministry (MITE) in the "CLYPEA-Innovation Network for Future Energy" framework, "subsoil deformations" project. We thank Mariano Grillo (General Director of DG ISSEG of the MITE), and his predecessors Gilberto Dialuce and Franco Terlizzese. We also thank Alessandra Fagiani.

Encouragement and continuous support by Carlo Doglioni, Andrea Morelli and Claudio Chiarabba were greatly appreciated. Thanks to Luisa Perini and Paolo Severi for fruitful discussions. Eni S.p.A. is acknowledged for kind provision of GNSS and Leveling data. Thanks to Topcon, Leica and the Emilia Romagna region for making available the GNSS data. Envisat and Sentinel-1 data are provided by European Space Agency. CSK® products are © ASI (Italian Space Agency), delivered under an ASI licence to use. Views and conclusions of the paper are those of the authors, and they should not be interpreted as representing official policies, either expressed or implied, of the Italian Government.

Appendix A. Supplementary material

Supplementary data to this article can be found online at https://doi.org/10.1016/j.jag.2022.102756.

References

Antoncecchi I., Rossi G., Ciccone F. et al., 2018. Multidisciplinary study on assessment of subsoil deformations caused by offshore hydrocarbon activity in Emilia Romagna region, aimed to develop a methodological approach for an integrated monitoring. Abstract in proceedings of 37° GNGTS, session 2.3, pp. 501-504.

Antoncecchi I., Rossi G., Ciccone F. et al., 2019. Studio Multidisiplinare delle deformazioni del suolo connesse alle attività di produzione di idrocarburi in aree dell'offshore emiliano romagnolo: avanzamento lavori. Abstract in proceedings of 36° GNGTS, session 2.3, pp. 513-517.

M. Antonellini, B.M.S. Giambastiani, N. Greggio, L. Bonzi, L. Calabrese, P. Luciani, L. Perini, P. Severi (2019). Processes governing natural land subsidence in the shallow coastal aquifer of the Ravenna coast, Italy, CATENA, Vol. 172, pp. 76-86, 10.1016/j.catena.2018.08.019.

Bitelli, G., Bonsignore, F., Unguendoli, M., 2000. Leveling and GNSS networks to monitor ground subsidence in the southern Po Valley. J. Geodyn. 30, 355–369.

Carminati, E., Martinelli, G., 2002. Subsidence rates in the Po Plain, northern Italy: the relative impact of natural and anthropogenic causation. Eng. Geol. 66 (3-4), 241–255. https://doi.org/10.1016/S0013-7952(02)00031-5.

Casu, F., Manzo, M., Lanari, R., 2006. A quantitative assessment of the SBAS algorithm performance for surface deformation retrieval from DInSAR data. Remote Sens. Environ. 102 (3-4), 195–210. https://doi.org/10.1016/j.rse.2006.01.023.

D'Agostino, N., Cheloni, D., D'Anastasio, E., Mantenuto, S., Selvaggi, G., 2008. Active tectonics of the Adriatic region from GPS and earthquake slip vectors. J. Geophys. Res. - Solid Earth. https://doi.org/10.1029/2008JB005860.

Dalla Via, G., Crosetto, M., Crippa, B., 2012. Resolving vertical and east-west horizontal motion from differential interferometric synthetic aperture radar: The L'Aquila earthquake. J. Geophys. Res. Solid Earth 117 (B2), n/a–n/a. https://doi.org/10.1029/2011JB008689.

Devoti, R., D'Agostino, N., Serpelloni, E., Pietrantonio, G., Riguzzi, F., Avallone, A., Cavaliere, A., Cheloni, D., Cecere, C., D'Ambrosio, C., Falco, L., Selvaggi, G., Métois, Marienne, Esposito, A., Sepe, V., Galvani, A., Anzidei, M., 2017. A Combined Velocity Field of the Mediterranean Region. Annals of Geophysics. https://doi.org/10.4401/ag-7059.

Devoti, R., Esposito, A., Pietrantonio, G., Pisani, A.R., Riguzzi, F., 2011. Evidence of large scale deformation patterns from GPS data in the Italian subduction boundary. Earth Planet. Sci. Lett. 311 (3–4, 15), 230–241. https://doi.org/10.1016/j.epsl.2011.09.034.

Devoti, R., Riguzzi, F., Cuffaro, M., Doglioni, C., 2008. New GPS constraints on the kinematics of the Apennines subduction. Earth Planet. Sci. Lett. 273 (1–2, 30), 163–174. https://doi.org/10.1016/j.epsl.2008.06.031.

Fuhrmann, T., Garthwaite, M.C., 2019. Resolving Three-Dimensional Surface Motion with InSAR: Constraints from Multi-Geometry Data Fusion. Remote Sens. 11, 241. https://doi.org/10.3390/rs11030241.

Gambolati G., Teatini P., 1998. Numerical Analysis of Land Subsidence due to Natural Compaction of the Upper Adriatic Sea Basin. In: Gambolati G. (eds) CENAS. Water Science and Technology Library, vol 28. Springer, Dordrecht. 10.1007/978-94-011-5147-4_5.

Gambolati, G, Teatini, P., Tomasi, L., Gonella, M., 1999. Coastline regression of the Romagna Region, Italy, due to natural and anthropogenic land subsidence and sea level rise. Volume35, Issue1 January 1999 Pages 163-184. 10.1029/1998WR900031.

Gonella M., Gambolati G., Giunta G., Putti M., Teatini P., 1998 Prediction of Land Subsidence Due to Groundwater Withdrawal along the Emilia-Romagna Coast. In: Gambolati G. (eds) CENAS. Water Science and Technology Library, vol 28. Springer, Dordrecht. 10.1007/978-94-011-5147-4_7.

Herring, T.A., Floyd, M.A., Perry, M., 2018. GAMIT/GLOBK for GNSS. GNSS Data Processing and Analysis with GAMIT/GLOBK and track Hotel Soluxe, Bishkek, Kyrgyzstan 2–7 July 2018.

Klemm, H., Quseimi, I., Novali, F., Ferretti, A., Tamburini, A., 2010. Monitoring horizontal and vertical surface deformation over a hydrocarbon reservoir by PSInSAR. First Break 28, 29–37. https://doi.org/10.3997/1365-2397.2010014.

E. Mantovani, M. Viti, D. Babbucci, C. Tamburelli, A. Vannucchi, F. Falciani, 2013. Assetto tettonico e potenzialità sismogenetica dell'Appennino Tosco-Emiliano-Romagnolo e Val Padana.

Montuori, A., Anderlini, L., Palano, M., Albano, M., Pezzo, G., Antoncecchi, I., Chiarabba, C., Serpelloni, E., Stramondo, S., 2018. Application and analysis of geodetic protocols for monitoring subsidence phenomena along on-shore hydrocarbon reservoirs. Int. J. Appl. Earth Obs. Geoinformation 69, 13–26. https://doi.org/10.1016/j.jag.2018.02.011.

Palano, M., Pezzo, G., Serpelloni, E., Devoti, R., D'Agostino, N., Gandolfi, S., Sparacino, F., Anderlini, L., Poluzzi, L., Tavasci, L., Macini, P., Pietrantonio, G., Riguzzi, F., Antoncecchi, I., Ciccone, F., Rossi, G., Avallone, A., Selvaggi, G., 2020. Geopositioning time series from offshore platforms in the Adriatic Sea. Scientific Data 7, 373. https://doi.org/10.1038/s41597-020-00705-w.

Pezzo, G., Petracchini, L., Devoti, R., Maffucci, R., Anderlini, L., Antoncecchi, I., Billi, A., Carminati, E., Ciccone, F., Cuffaro, M., Livani, M., Palano, M., Petricca, P., Pietrantonio, G., Riguzzi, F., Rossi, G., Sparacino, F., Doglioni, C., 2020. Active Fold-Thrust Belt to Foreland Transition in Northern Adria, Italy, Tracked by Seismic Reflection Profiles and GPS Offshore Data. Tectonics 39 (11). https://doi.org/10.1029/2020TC006425.

Serpelloni, E., Faccenna, C., Spada, G., Dong, D., Williams, S.D.P., 2013. Vertical GNSS ground motion rates in the Euro-Mediterranean region: New evidence of velocity gradients at different spatial scales along the Nubia-Eurasia plate boundary. JGR Solid Earth 118, 6003–6024. https://doi.org/10.1002/2013JB010102.

Serpelloni, E., Pintori, F., Gualandi, A., Scoccimarro, E., Cavaliere, A., Anderlini, L., Belardinelli, M.E., Todesco, M., 2018. Hydrologically Induced Karst Deformation: Insights From GPS Measurements in the Adria-Eurasia Plate Boundary Zone. J. Geophys. Res. Solid Earth 123, 4413–4430. https://doi.org/10.1002/2017JB015252.

Serpelloni, E., Vannucci, G., Anderlini, L., Bennett, L.A., 2016. Kinematics, seismotectonics and seismic potential of the eastern sector of the European Alps from GPS and seismic deformation data. Tectonophysics 688, 157–181. https://doi.org/10.1016/j.tecto.2016.09.026.

Teatini, P., Ferronato, M., Gambolati, G., Bertoni, W., Gonella, M., 2005. A century of land subsidence in Ravenna Italy. Environ. Geol. 47 (6), 831–846. https://doi.org/10.1007/s00254-004-1215-9.

Teatini, P., Ferronato, M., Gambolati, G., Gonella, M., 2006. Groundwater pumping and land subsidence in the Emilia-Romagna coastland, Italy: modeling the past occurrence and the future trend. Water Resour. Res. 42, W01406. https://doi.org/10.1029/2005WR004242.

Vasco, D.W., Wicks, C., Karasaki, K., Marques, 0., 2002. Geodetic imaging: reservoir monitoring using satellite interferometry. Geophys. Journ. Intern. 149, 555–571, 10.1046/j.1365-246X.2002.01569.x.
Werner, C., Wegmuller, U., Strozzi, T., Wiesmann, A., 2003. Interferometric point target analysis for deformation mapping. IEEE Int. Geosci. Remote Sens. 7, 4362–4364. https://doi.org/10.1109/IGARSS.2003.1295516.
Williams, S.D.P., 2008. CATS: GPS coordinate time series analysis software. GPS Solut. 12 (2), 147–153. https://doi.org/10.1007/s10291-007-0086-4.

Further reading

Zebker, H.A., Rosen, P.A., Goldstein, R.M., Gabriel, A., Werner, C., 1994. On the derivation of coseismic displacement fields using differential radar interferometry: the Landers earthquake. J. Geophys. Res. 99 (B10), 19617–19634. https://doi.org/10.1029/94JB01179.
https://unmig.mise.gov.it/index.php/it/).